Isothermal and nonisothermal crystallization of polymers: Analysis with a shear differential thermal analyzer

J. A. Martins,[a] Wd. Zhang, and A. M. Brito
IPC—Instituto de Polímeros e Compósitos, Universidade do Minho, Departamento de Engenharia de Polímeros, Campus de Azurém 4800-058 Guimarães, Portugal

U. Infante, M. Romero, and F. O. Soares
Universidade do Minho, Departamento de Electrónica Industrial, Campus de Azurém 4800-058 Guimarães, Portugal

(Received 16 March 2005; accepted 29 August 2005; published online 6 October 2005)

The working principle of an instrument developed for studying the effects of controlled shear pulses on the isothermal and nonisothermal solidification of polymers is presented. The device combines a capillary rheometer and a differential thermal analyzer (DTA). The capillary rheometer part of the system allows the production of shear pulses with controlled duration and intensity at any prescribed temperature up to 300 °C, and the DTA records the thermal effects resulting from the solidification. Results obtained for quiescent isothermal and nonisothermal crystallizations compare well with those obtained from power compensation differential scanning calorimetry. The effect of controlled shear pulses on the overall isothermal crystallization kinetics enables the evaluation of a critical strain responsible for the saturation of crystallization in sheared polymer melts. Additional shear (increase of the shear rate or of the shearing time) does not accelerate the crystallization kinetics. The shear-induced nonisothermal crystallization of polyethylene filled with talc shows the acceleration of the crystallization kinetics with the shear rate increase, thus confirming this device as a valuable experimental tool for studying the effect of shear on the solidification of fast crystallizing materials. © *2005 American Institute of Physics.* [DOI: 10.1063/1.2083087]

I. INTRODUCTION

Semicrystalline polymers are a group of materials with a broad range of commodities and engineering applications. From a morphological point of view, their solid state is characterized by spherulitic structures containing crystalline folded-chain lamellae and amorphous interlamellar regions. From a mechanical point of view, these materials may be viewed as a composite structure, with the crystalline phase conferring strength, and the amorphous phase, flexibility.

The quiescent crystallization of these materials has been studied at different morphological levels by several research groups with different model polymers. In this work, we will focus on the overall crystallization process. Here, the interest is the analysis of the overall transition kinetics from the liquid to the solid phase, and its temperature and cooling rate dependence.

It may be considered that both the quiescent isothermal and nonisothermal processes are reasonably well understood and physically described by model equations such as the Avrami/Komolgoroff[1,2] and Nakamura *et al.*[3] equations for isothermal and nonisothermal experiments, respectively. For example, it is possible to predict the average spherulite size by coupling experimental results of the spherulite growth rate and reciprocal of the half of crystallization time. This prediction can be made with reasonable accuracy for quiescent isothermal, nonisothermal, and also for processing experiments. For this last case, rotational molding was used and the average spherulite size was predicted for different sections of a plastic part 1 cm thick.[4]

Other processing technologies of these materials involve both thermal and flow fields. Therefore, the final microstructure prediction is more complicated than for quiescent crystallization processes. The analysis of elongational and shear flow fields, together with the strong temperature gradients found by these materials during their solidification, has also attracted the attention of several research groups.[5,6] The knowledge reached so far is that flow enhances crystallization due to a nucleation rate increase originated by distortions of the melt. This effect is further enhanced for higher molecular weight polymers. The saturation of shear was recorded for stresses higher than a critical value when they were applied during a time greater than a critical shearing time.[7] The development of long-lived oriented precursor structures during shear at temperatures higher than the nominal melting temperature was also observed.[7,8]

A key point, yet to be established, is the evaluation of the effect of flow conditions on the melt morphology and nucleation rate. Although some information about isothermal experiments was previously obtained for high crystallization temperatures,[6,7] more detailed experimental results are needed for an understanding and further modeling the overall phase change process. In addition, the shear-induced nonisothermal crystallization kinetics and experimental studies regarding the effect of shear on the overall crystallization of technologically important materials—namely, polymer

[a]Author to whom correspondence should be addressed.

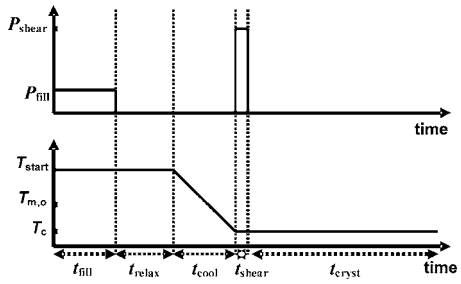

FIG. 1. Scheme of the experimental short-term shearing protocol proposed by Liedauer *et al.* (see Ref. 5). When the polymer is at a nominally isothermal temperature (crystallization temperature), a strong pressure pulse is applied during a short time implying the contact of material at the processing temperature with material at the crystallization temperature. The total strain imposed to the sample was limited in the experiments performed by these authors as well as in the experiments performed by Kumaraswamy *et al.* (see Ref. 6) to the length of the flow channel.

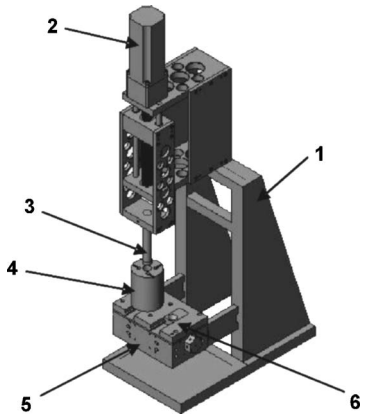

FIG. 2. General view of the shear DTA device. 1: holder; 2: servomotor; 3: piston; 4: accumulator; 5: cold block (contains the sample and reference ovens); 6: entrance valve of the reference channel.

nanocomposites—cannot be assessed with the existing experimental setups. Another important aspect is the separation of the nucleation resulting from the shear flow from the crystal growth of the formed nuclei.

To specifically deal with this last aspect, Liedauer *et al.*[5] implemented a newexperimental protocol, known as short-term shearing, which allows a separate control of the shear flow imposed to the melt and the temperature gradients in the sample. The experimental temperature-time and pressure-time protocol used for short-term shearing experiments is illustrated in Fig. 1. After filling a duct with the molten polymer at the processing temperature, and after allowing a relaxation time for erasing the polymer melt deformation resulting from the flow history, the duct is cooled to the isothermal crystallization temperature and a strong pressure pulse is applied for a short time. The maximum strain applied to the material analyzed is limited by the length of the flow channel. This experimental protocol was also used by Kumaraswamy *et al.*[6] with a small-sized setup that allows the use of smaller amounts of material and enables the use of the device in x-ray synchrotron facilities.

The shear differential thermal analyzer (DTA) device presented in this work[9,10] is capable of performing all the experiments described above, including short-term shearing. However, our main goal is to record the effects of the memory of shear during the isothermal and nonisothermal crystallization of polymers. Although the thermal recording of shear-induced crystallization was already performed,[11] and the working principle of the basic shear-DTA components is also known, their integration in a single device has not yet been accomplished. A detailed description of the working principles of the device and the results obtained are presented below.

II. THE SHEAR DTA WORKING PRINCIPLE

The shear DTA (Fig. 2) combines the capabilities of a DTA with a capillary rheometer. The system was conceived for enabling the further extension of the DTA to a power compensation differential scanning calorimeter (DSC), allowing the production of controlled shear pulses wherein the variables are the shear rate at the wall and the shearing time. The temperature difference between a sample (confined by the flow channel) and a reference (located in a similar channel) is monitored as a function of time and temperature. The device is capable of both isothermal and nonisothermal experiments. Shear pulses may be applied at any time during the sample thermal history—at the melting temperature, during the cooling, or at the crystallization temperature—as in the work of Liedauer *et al.*[5] and Kumaraswamy *et al.*[6]

The molten material, stored in an accumulator and maintained at the processing temperature, is pumped to the flow channel by the controlled movement of a piston (Fig. 2). By recording its initial and final position and controlling the time duration and speed of displacement, it is possible to know the flow rate of molten material pumped to the capillary, which allows the evaluation of the shear rate at the wall.

Once the sample's flow channel is filled, a protocol similar to that used by Liedauer *et al.*[5] and Kumaraswamy *et al.*[6] may be followed to analyze the effect of shear pulses on the polymer crystallization. However, a different protocol will be followed for studying the effect of memory of pulses with different duration and intensity on the overall crystallization kinetics. The shear pulse is applied at the processing temperature and not, as in the works mentioned previously, at the crystallization temperature (Fig. 3). Other work has also followed this protocol.[12] The overall crystallization kinetics is recorded by measuring the temperature difference between a sample and a reference, just as in a standard DTA.

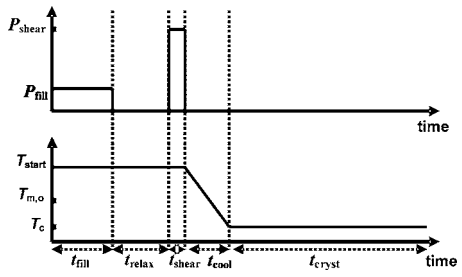

FIG. 3. Scheme of the experimental protocol used in this work for isothermal experiments. The shear pulse is applied at the processing temperature and the sheared melt is immediately cooled to the crystallization temperature.

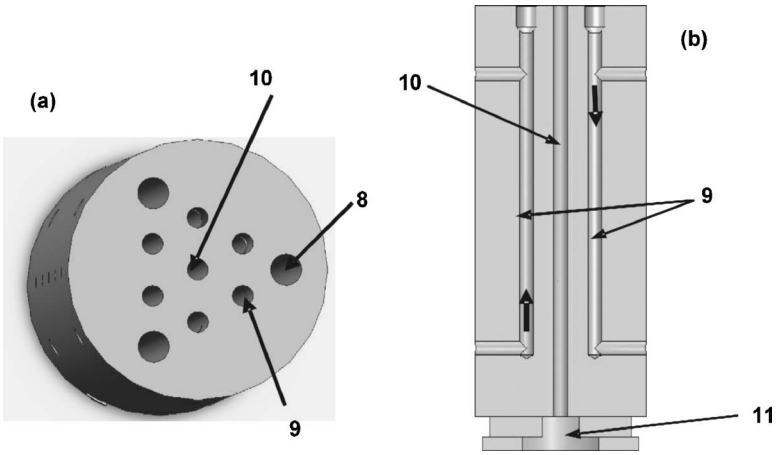

FIG. 4. View of the ovens. (a) Top view illustrating the disposition of the heating resistances and the cooling channels. 8: Heating resistances; 9: cooling channels; 10: flow channel. (b) Longitudinal cut illustrating the circulation of the cooling gas in adjacent cooling channels. The cooling channels (9) have a stopper at the top and the entrance of the cooling gas is made in a transversal direction to the flow channel; 11: exit valve.

III. INSTRUMENT DESIGN

A. Sample and reference ovens

The ovens are made from rods of AMPCOLOY 95®, Ampco® Metal, Portugal, with a diameter of 25 mm. This particular material was selected due to its high thermal conductivity (218 W/m K) and suitability for applications in molds for injection and blow molding. The length of each oven is 60 mm and a central channel with 2 ± 0.1 mm diameter was drilled along the length.

Each oven contains three 35 W heating resistances (CSS-1235/120V, Omega Engineering Inc., CT) positioned at 120° from each other around the capillary. Six cooling channels, each 2 mm in diameter and 60° from each other, were drilled along the length of the oven [Fig. 4(a)]. Their location in front of the heating resistances and behind the flow channel provides better temperature control during cooling experiments. The cooling is provided by nitrogen gas circulating in opposite directions in adjacent channels to ensure the temperature homogeneity along the length of the oven [Fig. 4(b)]. The gas flow rate in each channel is 5 cm^3/min.

Thermocouples (HKMTSS-010-G, Omega Engineering Inc., CT) are assembled transversally along the length of the channel. Figure 5 illustrates the arrangement of thermocouples in each oven, the placement of the heating resistances, and the aluminum heat sink block separating the sample and reference ovens. The block is cooled by a mixture of distilled water and ethylene glycol in equal proportions. The temperature of the liquid is controlled by a Julabo F12 refrigerated circulator (Julabo, UK).

B. Accumulator

A cylindrical hole (25 mm in diameter and 120 mm in length) was drilled in the accumulator block for storing the polymer pellets or powder. The heating power is supplied by cartridge heaters (CIR-3037/240, Omega Engineering Inc., CT) driven by a pulse width modulation power source (SCR71P-240-030-S60, Omega Engineering Inc., CT), which is controlled by a temperature controller (CNi16D53, Omega Engineering Inc., CT). The pressure at the bottom of the accumulator is measured with a pressure transducer (Dynisco PT460E, Dynisco Europe GmbH, Germany). The accumulator is thermally insulated from the cold block (containing the sample and reference ovens) by a glass-mica ceramic (8499K129, McMaster-Carr, IL).

C. Entrance and exit valves

An entrance valve controls the polymer melt flow to the sample oven. The purposes of this valve are twofold: (1) to promote the coupling between the accumulator and the capillary (open position) and (2) to maintain an effective thermal insulation between the accumulator, which is always at the polymer processing temperature, and the capillary (closed position). To fulfill this purpose, an aluminum conical channel was assembled over a rectangular glass-mica ceramic plate. The entrance valve is driven by a dc magnet (GL115E12, force: 100 N, stroke: 300 mm, Kendrion Magnettechnik GmbH, Germany), controlled at specific time intervals by the programmable logic controller (PLC) described below. The exit valve for the sample oven may work synchronously or asynchronously with the entrance valve of the same oven and is driven by another solenoid of the type indicated above.

To maintain the thermal symmetry between the sample and reference ovens, valves with the same design are assembled into the reference oven. The opening and closing of

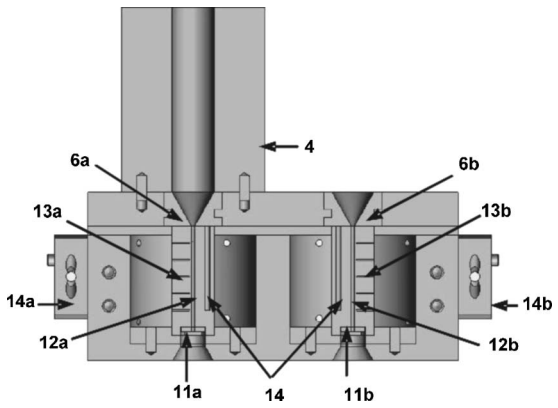

FIG. 5. Drawing of the accumulator and cold-block with the sample (a: left) and reference (b: right) ovens. 4: Accumulator; 6a and 6b: entrance valves to the sample and reference ovens; 11a and 11b: exit valves of the ovens; 12a and 12b: flow channel for the sample and reference; 13a and 13b: thermocouples for the sample and reference ovens; 14a and 14b: gas distributors for the sample and reference oven cooling channels.

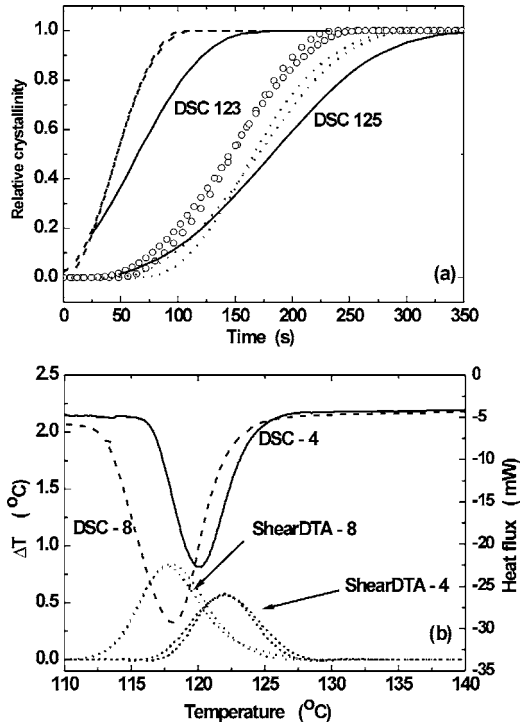

FIG. 6. Comparison of the results obtained for the isothermal (a) and nonisothermal (b) crystallization of polypropylene in the Perkin Elmer DSC-7 and in the shear DTA. (a) Solid line: quiescent DSC crystallization at 125 and 123 °C; the two dotted lines are the results obtained for the quiescent isothermal crystallization recorded in the shear DTA at 125 °C, while the two dashed lines are for the same results at 123 °C. The circles are the results of two experiments performed at 125 °C after a shearing at 230 °C for 60 s with an apparent shear rate at the wall of 12.9 s^{-1}. (b) Nonisothermal crystallization at the cooling rates indicated.

these "dead" valves is controlled manually. These operations are performed only when the reference oven is filled with reference silicon oil or when cleaning operations are performed.

D. Piston and servomotor

A servomotor (R88M-W75030H-BS1-B, Omron Corporation, Japan) with a rated torque of 2.39 N m at 3000 rpm and driven by a servodriver (R88D-WT08HH, Omron Corporation, Japan) is used for promoting the movement of the piston. The movement control is done through a position control unit (PCU) (NC133, Omron Corporation, Japan) controlled by the PLC.

The servomotor is coupled to a squared threaded power screw with a 2 mm pitch. The screw works with a bronze nut coupled to a rectangular block that is prevented from rotating by two guide pillars. The screw-nut kinematic couple converts the rotary motion of the servomotor shaft to linear motion of the rectangular block. This rectangular block is coupled to the piston. The overall arrangement is shown in Fig. 2.

The displacement accuracy is established by the pulses sent to the servodriver by the PCU. In a full screw turn the maximum number of pulses sent by the PCU is 2048, thus allowing a minimum displacement of the piston of 0.976 μm.

E. Instrumentation and software

General device control is done by a PLC (SYSMAG CS1G, Omron Corporation, Japan), which includes two thermocouple modules for the sample and reference ovens (PTS01, Omron Corporation, Japan), one digital module (OC226N), and the PCU previously mentioned. The digital module output drives the solenoids to close and open the valves of the sample oven.

The PLC also controls two power phase controllers (G3PX-220 EUN, Omron Corporation, Japan) and two temperature controllers (E5CK, Omron Corporation, Japan) for the sample and reference ovens. These temperature controllers receive from the PLC information of the temperature and time parameters and supply the power controller with the required signals for heating/cooling the ovens. Communication between the PLC and the temperature controllers is through a RS485 protocol.

A user-interface program, developed in Visual Basic, allows the selection of temperature-time steps [the time duration of the isothermal steps (when desired), heating or cooling rates], and the shear steps (number, time duration, and intensity).

F. Other device details

Assuming a maximum shear stress at the wall of the capillary of 0.1 MPa, the pressure drop in the capillary is 12 MPa. Since the pressure drops in the conical channel and accumulator are substantially lower, the total pressure drop is mainly that of the accumulator. With the basic setup, the tangential force developed at the screw by the servomotor is 159 N, implying a normal force of 7500 N and a pressure at the top of the accumulator of 15 MPa. To deal with fluids of higher viscosity (>4500 Pa s) the torque imposed on the screw may be increased by a factor of 10 (or higher) by inserting a gear reducer at the coupling between the motor and screw.

At the start of the experiment, the piston is moved to the zero (initial) position. The final position (L_f) is evaluated assuming a conservative flow from the accumulator through the capillary by selecting the desired apparent flow rate at the capillary wall ($\dot{\gamma}_{w,a}$) and the shearing time (t_{shear}),

$$L_f = L_i + \frac{R_c^2}{4R_a^2}\dot{\gamma}_{w,a}t_{\text{shear}}, \tag{1}$$

where R_c and R_a are the capillary and accumulator radius, respectively.

To ensure thermal homogeneity of the sample in the capillary, the temperature was measured at different points along the length of the channel. The flow profile in the capillary is stabilized in the first 6 mm at the entrance of the channel and in its remaining length the flow is a shear flow.

IV. RESULTS AND DISCUSSION

As in any regular thermal analysis device, a temperature calibration is required for accurate temperature measurements. Due to the impossibility of using standard metals for calibrating the shear DTA, liquid crystals usually used for calibrating DTA devices during cooling were selected. The

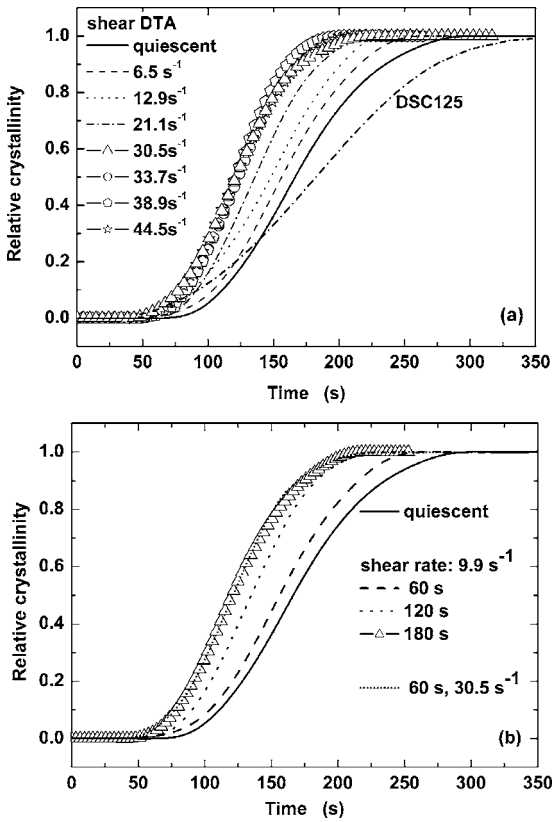

FIG. 7. Overall crystallization kinetics of iPP-isotactic polypropylene at 125 °C. (a) Effect of increasing shear rates applied at constant shearing time (60 s) on the isothermal crystallization. (b) Effect of increasing shearing time at constant (low) shear rate (9.9 s^{-1}). For comparison, (b) also shows the result obtained for the saturation at constant shearing time ($\dot{\gamma}_w = 30.5\ s^{-1}$, $t_{shear} = 60$ s), and for quiescent crystallization. The start temperature of the sheared melt was 230 °C. The shear rates at the wall and the shearing times are indicated in the figures. The saturation of crystallization occurs at an average strain of 1800 s.u.

liquid crystal 4-(4-Pentyl-cyclohexyl)benzoic acid-4-propyl-phenyl ester, (HP53, Merck) was used. The temperature onsets of two liquid-crystalline transitions at 68.2 and 93.9 °C were selected as the most appropriate. After a temperature calibration of each thermocouple, the difference in temperature recorded by adjacent thermocouples was within an accuracy of ±0.1 °C. In addition, a baseline of the device was obtained in the temperature range of the experiments, following the imposed temperature program with empty sample and reference ovens. This baseline may be stored as an independent file and subtracted during or after the experiment.

A key point for validating the experimental results obtained with any device is the analysis of the experimental reproducibility and its comparison with results obtained under the same conditions with other devices. Several polyolefins were studied with the shear DTA. The results shown below are for a polypropylene homopolymer (Moplen HP501M, Basel, Switzerland) having a melt flow index (MFI) (at 230 °C, 2.16 kg)=7.5 g/10 min according to ISO 1133.

Figure 6(a) shows the degree of conversion to the solid phase, obtained after peak integration, for quiescent isothermal crystallization at 123 and 125 °C. The polymer was previously molten at 230 °C and was cooled with a controlled cooling rate of −25 °C/min to the crystallization temperature. Similar results recorded with a Perkin Elmer DSC 7 are also indicated by solid lines. The difference in the crystallization kinetics between these devices may be ascribed to different sample thermal environments and also to the effect that different metal surfaces may have on the development of primary nuclei. Figure 6(a) also shows the effect of memory of a shear pulse applied at the molten temperature (230 °C), with a shear rate at the wall of 12.9 s^{-1} and a shearing time of 60 s, on the overall crystallization. The reproducibility of the experiments performed with the shear DTA is also indicated in Figs. 6(a) and 6(b) for isothermal and nonisothermal experiments, respectively.

The isothermal crystallization of polypropylene at 125 °C under quiescent conditions and after shearing the melt at 230 °C at constant shearing time (60 s) and with different shear rates from 6.5 s^{-1} up to 44.5 s^{-1} is shown in Fig. 7(a). The crystallization kinetics is accelerated with the shear rate increase until saturation. A saturation is also observed when a less intense shear pulse is applied to the melt for longer times (generating the same strain as that required for saturating the crystallization at shorter shearing times and high shear rates) [Fig. 7(b)]. For a crystallization temperature of 125 °C and a shearing melt temperature of 230 °C, the crystallization saturates at strains around 1800 s.u., measured with an error of 10% resulting from small variations on the cooling rate (it was not possible to guarantee a precise and uniform cooling rate for all experiments). This result clearly indicates that the total strain applied to the melt is the controlling factor in the saturation of shear-induced crystallization. This saturation was already observed in previous work,[7,12] and critical strains of similar magnitude were also measured.[12]

Since the nucleation density is limited for physical reasons (limited volume of material and finite dimensions of the critical nuclei), it is expected that the crystallization under shear should saturate. However, little or no attention has been given to the study of this phenomenon.[13] The critical strains responsible for the saturation of crystallization in sheared polymer melts can be evaluated with the shear DTA, allowing the analysis of how pre-existing orientation in the sheared molten polymers (including liquid crystals) affects the morphology and overall kinetics development.

To test the device sensitivity for studying the effect of controlled shear deformation on solidification of fast crystallizing materials, namely, polymer nanocomposites, the solidification of a low-density polyethylene (LDPE) filled with talc was examined. Polyethylene has fast crystallization kinetics and talc is known to be a strong nucleating agent. The material selected for this purpose was an LDPE (grade PE7324, Borialis, Portugal) having a MFI=3.3 g/10 min evaluated according to the norm ISO 1133 and thermodynamic melt temperature of 133.6 °C. For further enhancing the crystallization kinetics, shear pulses with time duration of 3 min and intensities (apparent shear rate at the wall) of 5 and 10 s^{-1} were applied during cooling from the melt (cooling rate −4 °C/min) in the temperature interval between 164 and 152 °C. The start temperature of the experiment was 190 °C. The results of Fig. 8 are, to our knowledge, the first

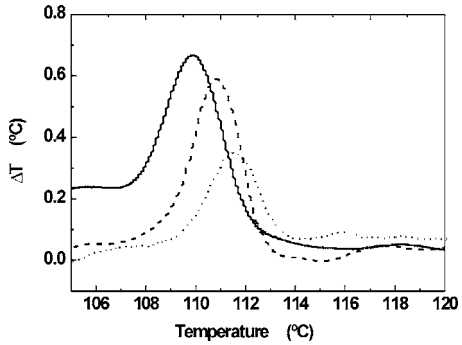

FIG. 8. Quiescent (solid line) and shear-induced nonisothermal crystallization experiments over a polyethylene sample. The sample cooling rate for the experiments indicated is −4 °C/min. Shear pulses with an apparent shear rate at the wall of 5 s^{-1} (dashed line) and 10 s^{-1} (dotted line) were applied during 3 min between 164 and 152 °C.

published results on the effect of controlled shear pulses on the nonisothermal crystallization of polymers and they show, together with the results indicated previously for the isothermal crystallization, that it is possible to record the sample temperature variation induced by those effects. The figure shows the expected acceleration of the crystallization with the applied shear rate. A saturation of the crystallization is also expected to occur for nonisothermal experiments. However, due to the combined effects of the cooling rate and shear pulse, the evaluation of the conditions leading to the saturation of the crystallization for these experiments is more complicated than for isothermal experiments.

ACKNOWLEDGMENTS

This was carried out under the project CTM/33061/2000 of the Portuguese Foundation for the Science and Technology (FCT) with funding from the POCTI and FEDER programs. FCT is also acknowledged by one of the authors (Wd. Z.) for the grant BPD/5517/2001. Rui Soares and Paralab Equipamentos Industriais e de Laboratório, S. A. are acknowledged by the support given to this work.

[1] M. Avrami, J. Chem. Phys. **8**, 212 (1940).
[2] A. N. Kolmogoroff, Izv. Akad. Nauk SSSR, Ser. Mat. **1**, 335 (1937).
[3] K. Nakamura, T. Watanabe, K. Katayama, and T. Amano, J. Appl. Polym. Sci. **16**, 1077 (1972).
[4] J. A. Martins, M. C. Cramez, M. J. Oliveira, and R. J. Crawford, J. Macromol. Sci., Phys. **B42**, 367 (2003).
[5] S. Liedauer, G. Eder, H. Janeschitz-Kriegl, P. Jerschow, W. Geymayer, and E. Ingolic, Int. Polym. Process. **8**, 236 (1993).
[6] G. Kumaraswamy, R. K. Verma, and J. A. Kornfield, Rev. Sci. Instrum. **70**, 2097 (1999).
[7] G. Kumaraswamy, A. M. Issaian, and J. A. Kornfield, Macromolecules **32**, 7537 (1999).
[8] R. H. Somani, L. Yang, and B. S. Hsiao, Physica A **304**, 145 (2002).
[9] J. A. Martins, A. M. Brito, M. Romero, F. O. Soares, and U. Infante, Patent No. 103157, Portugal (2004).
[10] J. A. Martins, Wd. Zhang, A. M. Brito, U. Infante, F. O. Soares, and M. Romero, Macro 2004, Paris (www.e-polymers. org/paris/data/L3903.pdf)
[11] W. Nagatake, T. Takahashi, Y. Masubuchi, J.-I. Takimoto, and K. Koyama, Polymer **41**, 523 (2000).
[12] C. K. Chai, Q. Auzoux, H. Randrianatoandro, P. Navard, and J. M. Haudin, Polymer **44**, 773 (2003).
[13] H. Janeschitz-Kriegl, Colloid Polym. Sci. **281**, 1157 (2003).